iScience, Volume *25*

Supplemental information

MASTL is enriched in cancerous and pluripotent stem cells and influences OCT1/OCT4 levels

Elisa Närvä, Maria E. Taskinen, Sergio Lilla, Aleksi Isomursu, Mika Pietilä, Jere Weltner, Jorma Isola, Harri Sihto, Heikki Joensuu, Sara Zanivan, Jim Norman, and Johanna Ivaska

A

	n	MASTL Negative	MASTL Positive	chi-square test P
Age (years)	851			
Median (51)		51	50	0.0800
Tumor size (mm)	839			
Median (12)		22	22	0.5370
N.A.				
Ki-67 (%)	794			
Median (19.6)		17.1	38.2	0.0001
N.A.	57			
Tumor size				
pT1	362	292 (80.7)	70 (19.3)	0.4940
pT2	418	334 (79.9)	84 (20.1)	
pT3 or pT4	71	61 (85.9)	10 (14.1)	
Nodal status				
pN0	87	63 (72.4)	24 (27.6)	0.0380
pN+	764	624 (81.7)	140 (18.3)	
Histological grade				
1	117	108 (92.3)	9 (7.7)	
2	341	283 (83.0)	58 (17.0)	
3	357	262 (73.4)	95 (26.6)	0.0001
N.A.	36			
Tumor histology				
Ductal	674	523 (77.6)	151 (22.4)	0.00001
Lobular	158	150 (94.9)	8 (5.1)	
Special type	19	14 (73.7)	5 (26.3)	
p53				
Negative	620	401 (84.0)	217 (16.0)	
Positive	208	103 (70.2)	108 (29.8)	0.0001
N.A.	23			

FinHer Breast cancer series

B

	n	ITGB3 Negative	ITGB3 Positive	chi-square test P
Primary tumor size				
pT1	314	273 (86.9)	41 (13.1)	0.024
pT2-4	447	361 (80.8)	86 (19.2)	
Nodal status				
negative	85	60 (70.6)	25 (29.4)	0.001
positive	675	573 (84.9)	102 (15.1)	
N.A.	1	1	0	
Histological type				
Ductal	607	490 (80.7)	117 (19.3)	0.001
Lobular	137	127 (92.7)	10 (7.3)	
Special type	17	10 (100)	0	
Histological grade				
Grade 1	95	89 (93.7)	6 (6.3)	
Grade 2	307	269 (87.6)	38 (12.4)	0.001
Grade 3	328	248 (75.6)	80 (24.4)	
N.A.		28	3	
ER status				
Positive	530	477 (90.0)	53 (10.0)	0.001
Negative	231	157 (68.0)	74 (32.0)	
PR status				
Positive	432	392 (90.7)	40 (9.3)	0.001
Negative	328	241 (73.5)	87 (26.5)	
N.A.		1	0	
HER2 status (CISH)				
Negative	587	503 (85.7)	84 (14.3)	0.001
Positive	174	131 (75.3)	43 (24.7)	
Ki-67				
≤15%	238	211 (88.7)	27 (11.3)	0.001
>15%	436	343 (78.7)	93 (21.3)	
N.A.	87	80	7	
p53				
Negative	543	468 (86.2)	75 (13.8)	0.001
Positive	197	145 (73.6)	52 (26.4)	
N.A.	21	21	0	

FinHer Breast cancer series

C

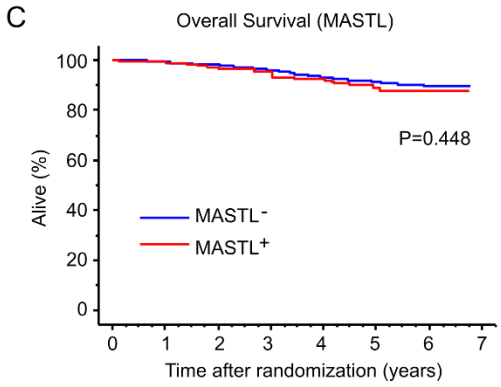

Figure S1. MASTL expression correlates with β3-integrin (ITGB3)-positive breast cancers, Related to Figure 1. **A)** Patient median age, breast tumour size, Ki-67 expression, histological grade/type, p53 expression, and axillary nodal status among MASTL-negative and -positive patients in the FinHer series. **B)** Tumour size, axillary nodal status, histological type/grade, hormone receptor (ER, PR) expression, HER2 status, Ki-67 expression, and p53 expression among ITGB3-negative and -positive patients. **C)** Survival of FinHer patients with negative (MASTL-), or high (MASTL+) MASTL expression. Kaplan–Meier survival-table method and log-rank test.

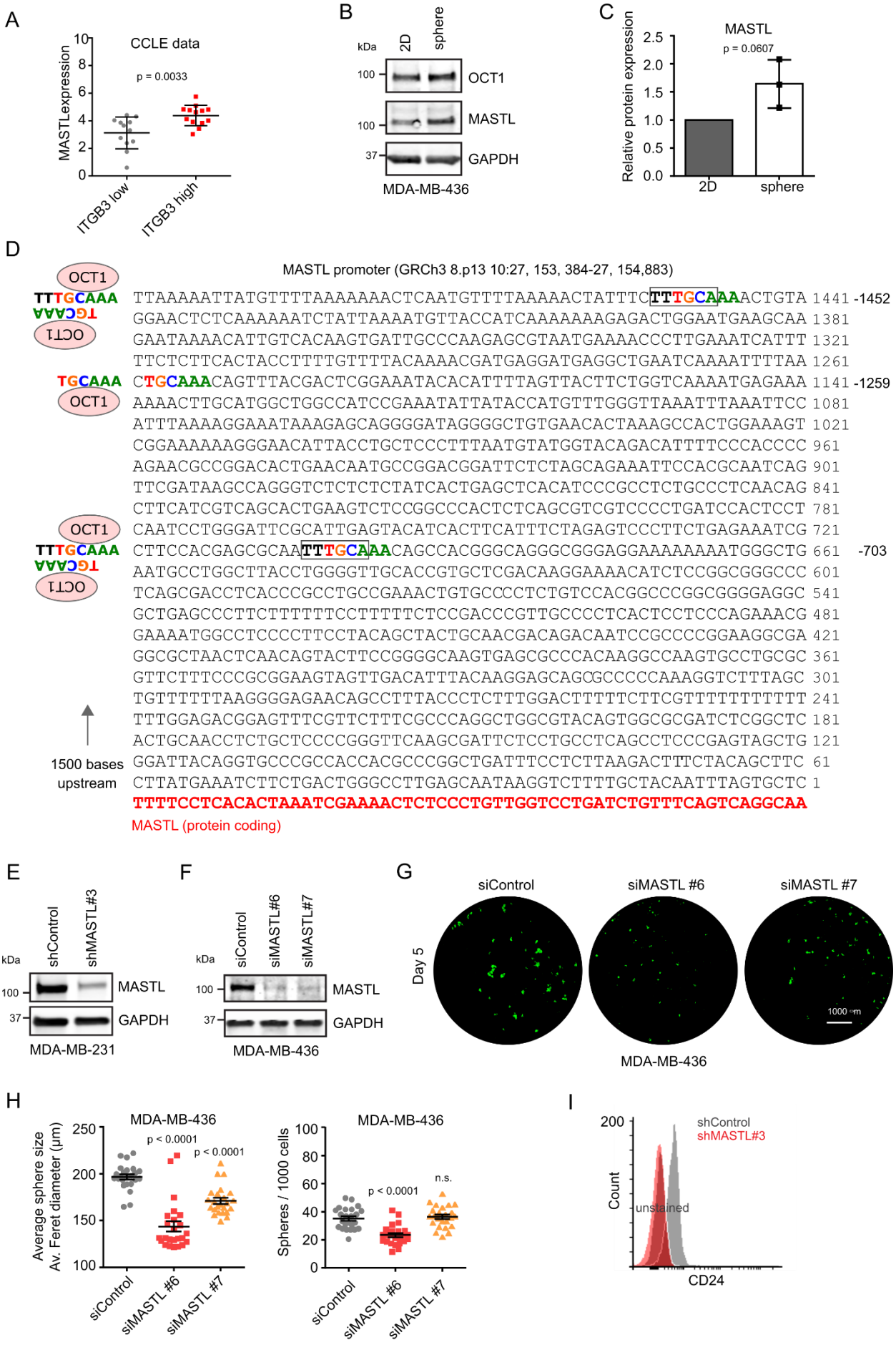
A
CCLE data
p = 0.0033
MASTLexpression
ITGB3 low
ITGB3 high
B
kDa
2D
sphere
OCT1
MASTL
GAPDH
MDA-MB-436
C
MASTL
p = 0.0607
Relative protein expression
2D
sphere
D
MASTL promoter (GRCh3 8.p13 10:27, 153, 384-27, 154,883)
OCT1
TTTGCAAA
TGCAAA
-1452
-1259
-703
1500 bases upstream
MASTL (protein coding)
E
shControl
shMASTL#3
MASTL
GAPDH
MDA-MB-231
F
siControl
siMASTL#6
siMASTL#7
MASTL
GAPDH
MDA-MB-436
G
siControl
siMASTL #6
siMASTL #7
Day 5
1000 µm
MDA-MB-436
H
MDA-MB-436
Average sphere size
Av. Feret diameter (µm)
p < 0.0001
p < 0.0001
siControl
siMASTL #6
siMASTL #7
MDA-MB-436
Spheres / 1000 cells
p < 0.0001
n.s.
I
shControl
shMASTL#3
unstained
Count
CD24

Figure S2. High MASTL levels correlate with OCT1 and mammosphere formation, Related to Figure 2. A) MASTL expression in breast cancer cell lines with high or low ITGB3 expression based on Cancer Cell Line Encyclopedia (CCLE) data, unpaired t-test. **B)** Western blotting of OCT1, MASTL, and GAPDH in MDA-MB-436 cells grown as a monolayer (2D) or in mammosphere culture conditions. **C)** Relative protein expression of MASTL to GAPDH, experimental setup shown in A. (n=3 biologically independent experiments, unpaired t-test, mean ± SD). **D)** Predicted binding sites for OCT1 in the promoter region of MASTL based on the consensus binding sequence TGCAAA. **E)** Western blotting of MASTL and GAPDH in tetracycline-inducible shControl or shMASTL#3 MDA-MB-231 cells pretreated with tetracycline (1 µg/ml) for 5 days. **F)** Western blotting of MASTL and GAPDH in siControl, siMASTL#6 and siMASTL#7 treated MDA-MB-436 cells after 48 hours. **G)** Representative images of siControl, siMASTL#6 and siMASTL#7 treated MDA-MB-436 cells grown 5 days in mammosphere culture conditions and stained with Calcein (Nikon Eclipse Ti-E widefield microscope, Hamamatsu Orca C13440 Flash 4.0 ERG [b/w] sCMOS camera and Plan Apo lambda 20×/0.80, WD 1,000-µm objective). **H)** Average mammosphere size (average ferret diameter of spheres in µm) and sphere number/1000 cells plated, experimental setup shown in E. (n=3 biologically independent experiments, 8 replicate wells/experiment, unpaired t-test, mean ± SEM). **I)** Representative flow cytometry histograms of CD24 expression in tetracycline-induced (4 days) shControl and shMASTL#3 MDA-MB-231 cells.

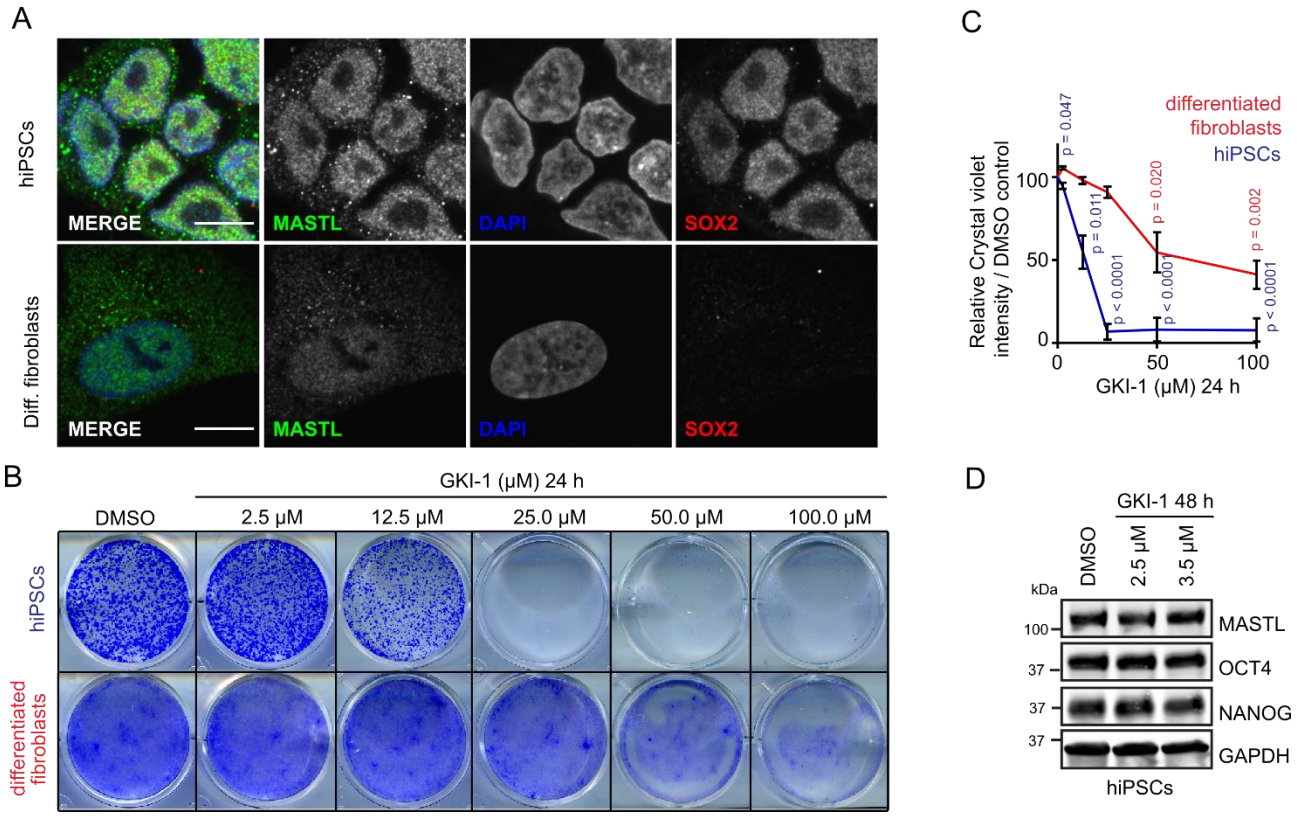

Figure S3. MASTL is highly expressed in pluripotent stem cells and supports pluripotency, Related to Figure 3. A) Immunostaining of MASTL, SOX2 (pluripotency indicator), and DAPI in hiPSCs and in differentiated fibroblasts, Scale bar, 10 µm. **B)** Crystal violet staining of hiPSC colonies and differentiated fibroblasts treated with DMSO or GKI-1 (2.5-100 µM) for 24h. **C)** Relative Crystal violet intensity**,** experimental setup shown in E. (n=3 biologically independent experiments, unpaired t-test, mean ± SEM). **D)** Western blotting of MASTL, OCT4, NANOG, and GAPDH in hiPSCs treated with DMSO or GKI-1 (2.5-3.5 µM) for 48h.

A

Gene name	mRNA	total proteome	surfaceome	Protein name
SLC2A3	-2.22	-2.22	-1.85	GLUT3
ESAM	-0.96	-0.98	-0.94	Endothelial cell-selective adhesion molecule
ANO6	N.A	N.A	-0.87	Anoctamin-6
TUBB6	-0.53	-0.71	-0.83	Tubulin beta-6 chain
FZD6	N.A	-0.71	-0.81	Frizzled-6
SLC44A1	-0.50	-0.71	-0.73	Choline transporter-like protein 1
ICAM1	N.A	-0.63	-0.69	intercellular adhesion molecule 1
ATP2A2	-0.95	-0.79	-0.67	endoplasmic reticulum calcium ATPase2
SLC20A1	N.A	-0.66	-0.67	sodium-dependent phosphate transporter 1
TGFBR2	-0.74	-0.61	-0.61	TGF-beta receptor type-2
IPO5	-0.83	-0.61	-0.57	Importin-5
SUSD5	N.A	N.A.	0.62	Sushi domain-containing protein 5
PLXDC2	N.A	0.84	0.68	Plexin domain-containing protein 2
INSR	N.A	N.A.	0.69	Insulin receptor
F11R	N.A	N.A.	0.69	Junctional adhesion molecule A
EPHA4	N.A	N.A.	0.97	Ephrin type-A receptor

Figure S4. MASTL depletion influences stem-cell-associated surface proteins, Related to Figure 4. A) Comparison of the significantly altered surface proteins, surfaceome (SILAC siMastl/siControl Ratio >0.5/<-0.5) to previously published (Taskinen et al., 2020) transcriptional changes, mRNA, (FDR < 0.05) measured with Illumina HT-12 and total protein levels, proteome (SILAC siMastl/siControl Ratio (log_2) >0.5/<-0.5) in MASTL-silenced cells. N.A (not applicable based on the parameters set in the analysis).

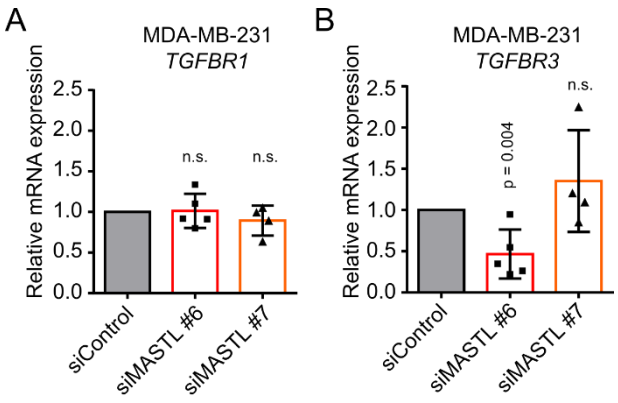

Figure S5. MASTL effect on TGFBR1 and TGFBR3, Related to Figure 5. A-B) Relative mRNA expression of TGFBR1 or TGFBR3 in siControl, siMASTL#6 and siMASTL#7 treated MDA-MB-231 cells after 48 hours (n=4-5 biologically independent experiments, unpaired t-test, mean ± SD).